Lukas Pavlasek, Martin Bernatik, Jan Trojan

Effect of Higher Contents of Manganese and Magnesium on the Mechanical Properties of Twin-Roll Cast Aluminium Alloy EN AW-8011

Abstract: Because of their excellent formability and sufficient mechanical properties, aluminium alloys based on an aluminium–iron–silicon system are very popular materials, commonly used in the production of thin foils. Alloy EN AW-8011 contains approximately 0.50–1.00 wt. % of iron and 0.40–0.80 wt. % of silicon. The other elements, including manganese and magnesium, are present only as impurities. However, these two elements are generally very effective enhancers of mechanical properties. Due to their very low concentrations in alloy EN AW-8011, the influence of manganese and magnesium on mechanical properties is often overlooked. In the research work discussed in the article, the properties of two Twin-Roll cast aluminium alloy EN AW-8011 containing various amounts of manganese and magnesium were investigated using optical microscopy, scanning electron microscopy (SEM), energy dispersive X-ray analysis (EDX) and tensile tests. The test results revealed that higher contents of magnesium and manganese significantly changed the mechanical properties of the alloy.

Key words: EN AW-8011, twin-roll casting (TRC), manganese, magnesium, mechanical properties

DOI: 10.32730/mswt.2024.68.4.3

1. Introduction

Aluminium alloys of the 8xxx series can be heat-treatable or non-heat-treatable. For example, alloys based on aluminium-lithium or aluminium-scandium systems are heat-treatable and used, e.g. in the aerospace industry. However, the most commonly used 8xxx series alloys are based on the aluminium–iron binary system and are non-heat-treatable [1–2].

Iron and silicon are often considered to be unfavourable impurities in commercial aluminium alloys [3–4], yet in the case of 8xxx series alloys, they are alloyed deliberately. Owing to the alloying of iron and silicon, the mechanical properties (tensile strength and yield strength) of 8xxx series alloys are higher than those of 1xxx series aluminium alloys. In addition, the formability of these materials is still excellent making them usable in the fabrication of thin foils [5–7]. Aluminium foils made of alloys EN AW-8079, EN AW-8011 and EN AW-8006 are used in many industrial applications such as packaging (household foil, drug packaging, etc.) or in heat-exchanger systems (the so-called mechanical finstocks) [5–7].

The solubility of iron in aluminium is very low (0.05 wt. % at 650°C [8–9]) which means that it precipitates into secondary phases such as Al_3Fe, $Al_{13}Fe_4$ (stable) or Al_6Fe, Al_mFe and Al_xFe_y (metastable) [5–6, 10]. Although the solubility of silicon in aluminium is higher, silicon has a strong tendency to form ternary phases with aluminium and iron, such as α-AlFeSi (Al_8Fe_2Si or $Al_{12}Fe_3Si$) and β-AlFeSi (Al_5FeSi or Al_9Fe_2Si). This tendency even growths in cases of homogenization. During homogenization, silicon from the aluminium matrix can diffuse into Al–Fe phases and transform them into AlFeSi phases [5, 7, 10–12].

The situation becomes even more complicated in the presence of manganese, which is very effective in the strengthening of aluminium alloys through the solid solution. However, the solubility of manganese is limited (1.40 wt. % at 650°C; [8–9]), which means that it precipitates into phases. One of the stable phases is Al_6Mn, yet this phase is not formed in terms of 8xxx series aluminium alloys. Instead, manganese and iron can act as substitutes for each other, leading to the appearance of complex phases such as $Al_6(MnFe)$, α-Al(FeMn)Si and β-Al(FeMn)Si. The formation of phases containing manganese reduces the role of this element in solid solution strengthening [7].

The presence of manganese must be taken into account when preparing the material using the Twin-Roll Casting (TRC) technology. In the TRC process, the material is cast between two intensively water-cooled rolls. A very high cooling rate results in the formation of a supersaturated metastable matrix in the as-cast state [13]. During the TRC process, manganese forms a very fine dispersion of intermetallic phases, which are overly small and, consequently, insufficient to act a nuclei for grains during the recrystallization process. In cases of higher manganese contents in 8xxx series aluminium alloys, the process of homogenization is often used in order to create larger particles which could be sufficient recrystallization nuclei [1, 13–15].

Another problematic element is magnesium. This element is responsible for an increase in mechanical properties (YS, UTS) (magnesium is 1.5 times more effective than manganese) [1]. However, the amount of magnesium is usually strictly controlled in packaging foils made of 8xxx series aluminium alloys. Magnesium modifies the surface layers of finished products (aluminium foils) by creating MgO and thus impairs the adhesion of varnish used in the food-packaging industry [16].

Lukas Pavlasek – VSB – Technical University of Ostrava, Faculty of Material Science and Technology, AL INVEST Břidličná, a.s. (Republika Czeska); Martin Bernatik, Jan Trojan – AL INVEST Břidličná, a.s. (Republika Czeska)
Corresponding author: lukepav@email.cz

Although the 8xxx series aluminium alloys are widely used in industry, the correlation between mechanical properties and small changes in the chemical composition has not yet been fully described. This work compares the mechanical properties of two TRC aluminium alloys EN AW-8011 containing various amounts of magnesium and manganese and aims to investigate the influence of these elements on the mechanical properties of aluminium foils (or thin sheets) at various processing stages.

2. Material and methods

Two samples of alloy EN AW-8011 with different manganese and magnesium contents were prepared by the AL INVEST Břidličná company. The material was obtained using the Twin-Roll Casting technology and, next, processed (using the standard industrial route) into sheets having a thickness of 0.3 mm (in the as-delivered state). The chemical composition of both alloys was determined using the iSPARK quantometer. The samples were taken from the melt during production. The chemical composition of the samples is presented in Table 1.

Afterwards, the samples were annealed in the LAC laboratory furnace. The first set of samples was homogenized, whereas the second set was annealed in order to obtain the recrystallized grain structure.

The heat treatment parameters are presented in Fig. 1.

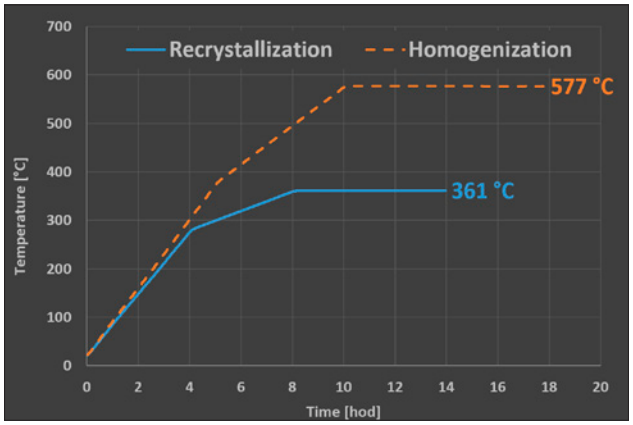

Fig. 1. Heat treatment regime

After heat treatment, the samples were cold-rolled [using KALMAQ laboratory rolling mill (see Fig. 2) to their final thickness.

The reductions of all samples are presented in Tables 2 and 3 (the variation in reductions amounted to approximately ± 5%).

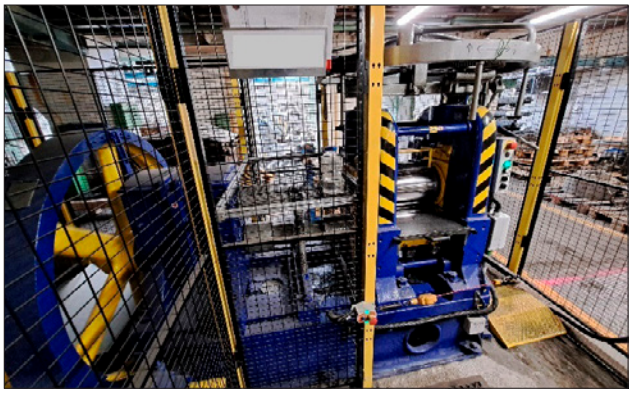

Fig. 2. KALMAQ laboratory rolling mill

At every processing stage, the samples were subjected to tests of mechanical properties and metallographic observations. The mechanical properties were examined in accordance with the ISO 6892-1 [17] standard using TIRA and INSTRON tensile test machines.

Table 2. Reduction of the high-alloyed samples

High-alloyed samples			
Sample	**Initial thickness [mm]**	**Final thickness [mm]**	**Reduction [%]**
AS-DELIVERED	0.29	0.29	0
RECRYSTALLIZED	0.29	0.29	0
HOMOGENIZED	0.29	0.29	0
REC. + 25% DEF.	0.29	0.22	24.14
HOM. + 25% DEF.	0.29	0.225	22.41

Table 3. Reduction of the low-alloyed samples

Low-alloyed samples			
Sample	**Initial thickness [mm]**	**Final thickness [mm]**	**Reduction [%]**
AS-DELIVERED	0.29	0.29	0
RECRYSTALLIZED	0.29	0.29	0
HOMOGENIZED	0.29	0.29	0
REC. + 25% DEF.	0.29	0.23	20.69
HOM. + 25% DEF.	0.29	0.205	29.31

Table 1. Chemical composition of the samples compared to EN 573-3(A1)

Sample	**Si [%]**	**Fe [%]**	**Cu [%]**	**Mn [%]**	**Mg [%]**	**Cr [%]**	**Zn [%]**	**Ti [%]**	**Others**		**Al [%]**
									each [%]	**total [%]**	
High-alloyed	0.7391	0.6104	0.0097	0.0863	0.0601	0.0029	0.0271	0.0184	x	0.0368	98.4092
Low-alloyed	0.6201	0.6436	0.0072	0.0095	0.0023	0.0011	0.0034	0.0251	x	0.0290	98.6587
EN AW-8011 (EN 573-3)	0.40–0.80	0.50–1.00	<0.10	<0.10	<0.10	<0.10	<0.10	<0.05	<0.05	<0.15	Bal.

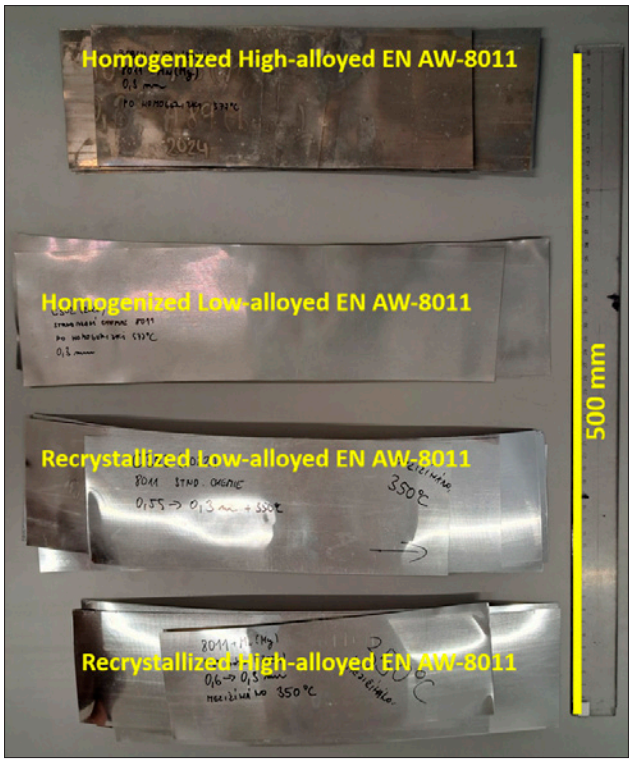

Fig. 3. Samples after heat treatment

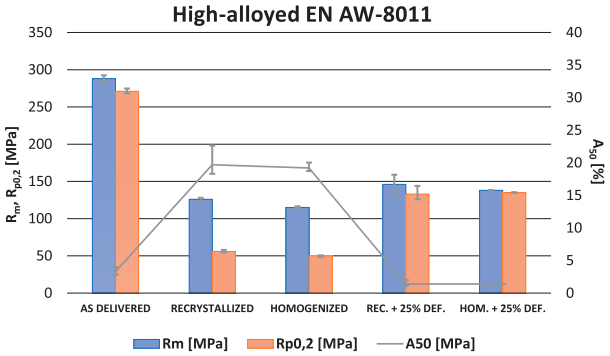

Fig. 4. Mechanical properties of the high-alloyed samples (longitudinal). (Note: Only 1 measurement was performed in terms of HOM. + 25% DEF. sample.)

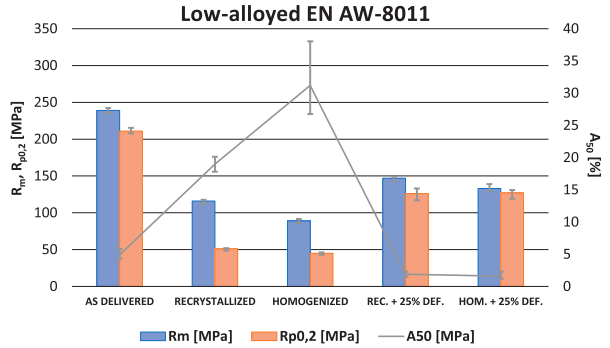

Fig. 5. Mechanical properties of the low-alloyed samples (longitudinal)

The samples used in metallographic tests were subjected to grinding and polishing and, afterwards, were analysed using a Thermo Scientific Scanning Electron Microscope (SEM) and an OLYMPUS GX 53 Optical Microscope (OM). The samples were etched in the standard hydrofluoric acid solution (in order to analyse intermetallic phases) and etched electrolytically in the standard fluoroboric acid solution (in order to analyse the grain structure, which was observed using the polarized light mode). The average grain size was determined in accordance with the ASTM E112-10 standard [18].

3. Results and discussion

The samples after various annealing processes is presented in Fig. 3.

Both recrystallized samples contained shiny metallic surfaces which were very similar to each other. In contrast, the surfaces of the homogenized samples differed in relation to both variants of EN AW-8011. The surface of the high-alloyed sample (higher manganese and magnesium contents) was significantly darker than that of its low-alloyed counterpart. The primary reason for the aforesaid situation could be the modification of the surface layer by magnesium (leading to the formation of magnesium oxide) [16].

The mechanical properties of the samples are presented in Fig. 4 and Fig. 5. A significant difference in the mechanical properties could be seen in relation to each stage of processing. The samples containing manganese and magnesium were characterised by significantly higher yield points (strength) ($Rp_{0.2}$) and the ultimate tensile strength (R_m) than those of the samples having low contents of the aforesaid elements. On the other hand, the values of elongation ($A_{50/100}$) were nearly the same between as regards the high-alloyed and low-alloyed variants. The only exception was the state after homogenization, where elongation was 1.6 times higher than that obtained in relation to low-alloyed EN AW-8011.

This difference was considered a surprise as the high-alloyed sample was characterised by nearly the same mechanical properties in the recrystallized and homogenized state, whereas the properties (esp. elongation) of the low-alloyed sample differ significantly between the above-named states. It should be noted that measurement deviation was quite significant in terms of the homogenized low-alloyed sample (see Fig. 5).

Figures 6–10 present the microstructure (phases) of the recrystallized and homogenized samples (OM and SEM). All the Figures were captured in the longitudinal direction.

Figure 6 reveals the difference in the phase morphology of the samples after recrystallization and homogenization. The lower temperature during recrystallization was insufficient to activate transformations strong enough to significantly modify the phase morphology. The phases were still elongated in the rolling direction [13–15].

However, at the higher temperature and longer time, diffusion accelerated and the morphology of the phases changed towards more rounded (which could be confirmed by EDX mapping). The distribution of selected elements is presented in Figures 7–10. For better clarity, only the maps of aluminium, iron, silicon, manganese and magnesium are presented in the publication. As can be seen from the distribution of silicon in the recrystallized state, the counts for silicon are mostly concentrated in the intermetallic phases. On the other hand, in the homogenized state, the silicon counts are also present in the α-(Al) matrix, indicating the diffusion of silicon from the phases into the matrix [6]. It should also be noted that the counts for magnesium and manganese do not seem to concentrate in the phases and are uniformly dispersed throughout the Figure. Therefore, it could be concluded that both elements probably remained in the solid solution.

Although there were differences in the shape of the phases between the recrystallized and the homogenized state, no significant changes were observed between corresponding high-alloyed and low-alloyed samples. Nevertheless, the phases in the high-alloyed variant seem to be finer and more uniformly dispersed.

Figures 11–12 show the grain structures of the samples in the recrystallized and homogenized state. The average grain size is presented in Table 4. It can be easily seen that the homogenized low-alloyed sample is characterised by coarser grain structure if compared to its high-alloyed counterpart. This could be partly explained by the varying distribution and coarseness of the phases. In terms of the low-alloyed homogenized samples, the difference in the grain size could trigger the different behaviour of the sample during the tensile test [13–15].

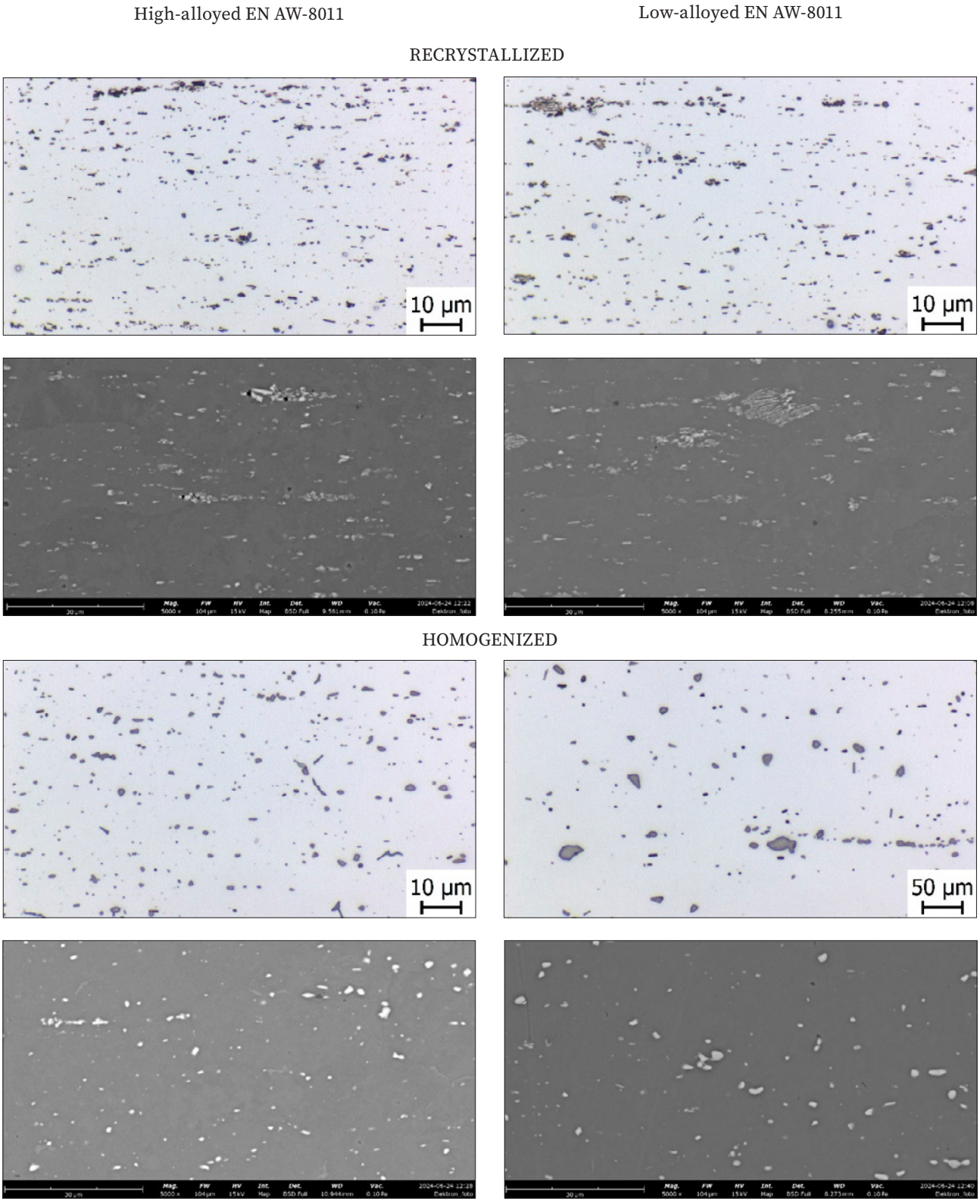

Fig. 6. Microstructure (phases) of the recrystallized and homogenized samples (longitudinal)

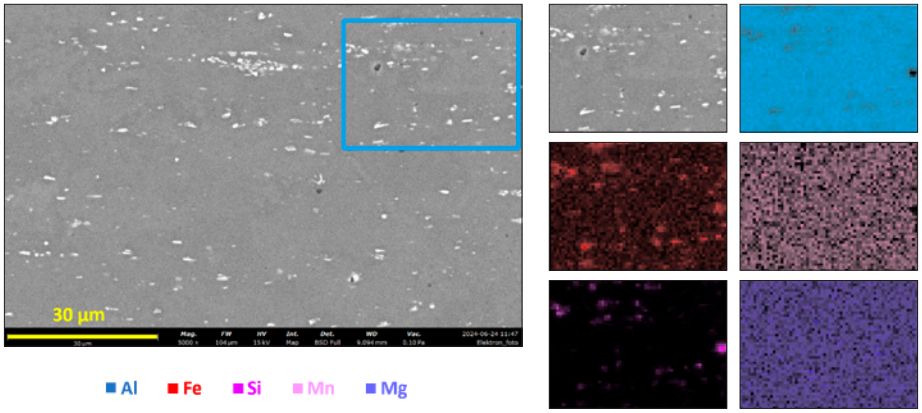

Fig. 7. Mapping (EDX) of phases in high-alloyed EN AW-8011 after recrystallization

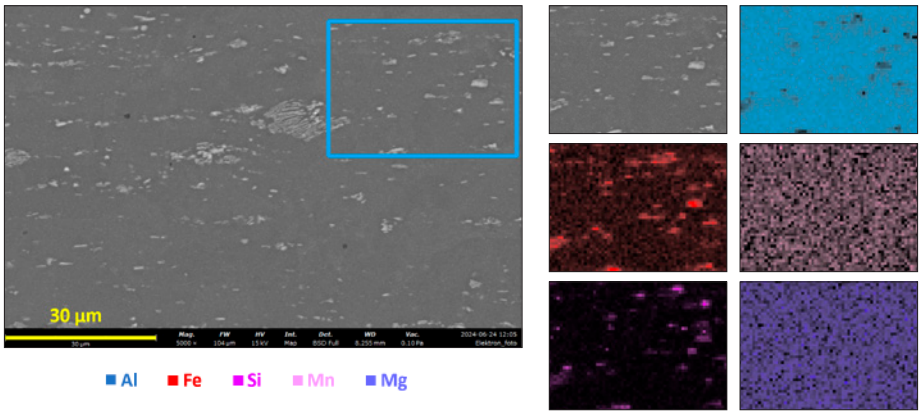

Fig. 8. Mapping (EDX) of phases in low-alloyed EN AW-8011 after recrystallization

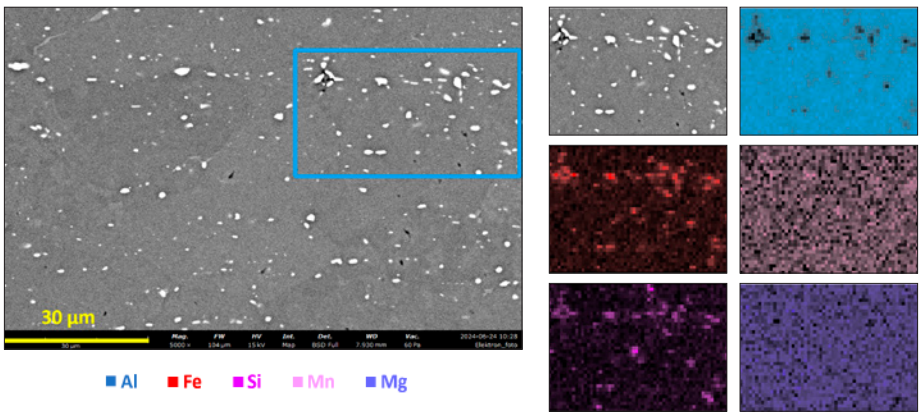

Fig. 9. Mapping (EDX) of phases in high-alloyed EN AW-8011 after homogenization

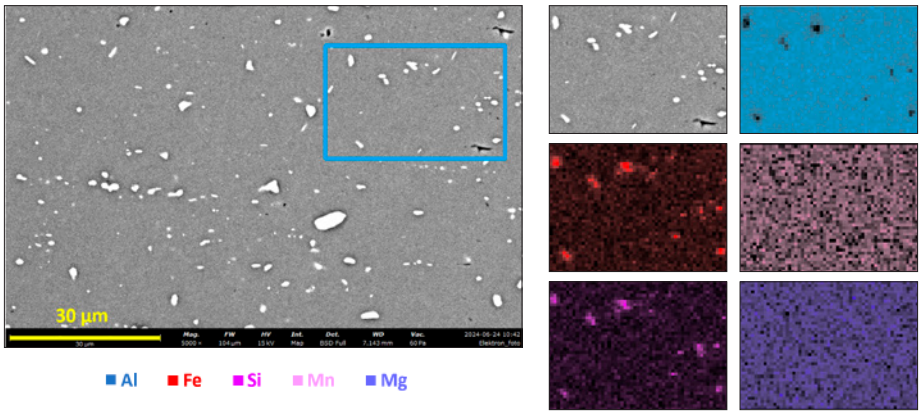

Fig. 10. Mapping (EDX) of phases in low-alloyed EN AW-8011 after homogenization

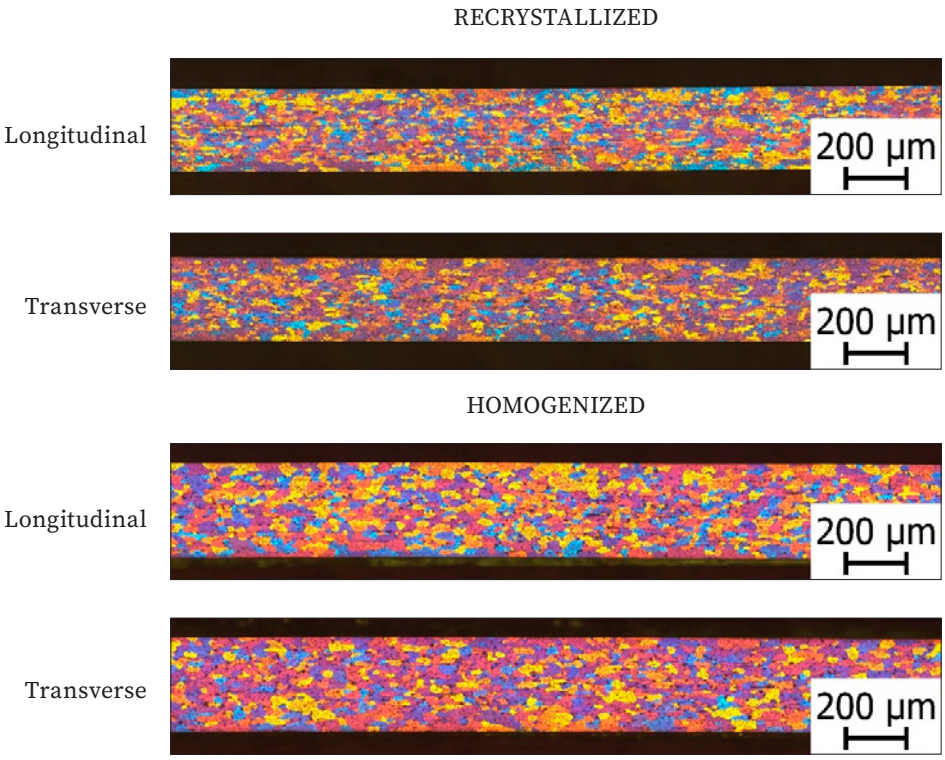

Fig. 11. Grain structure of high-alloyed EN AW-8011

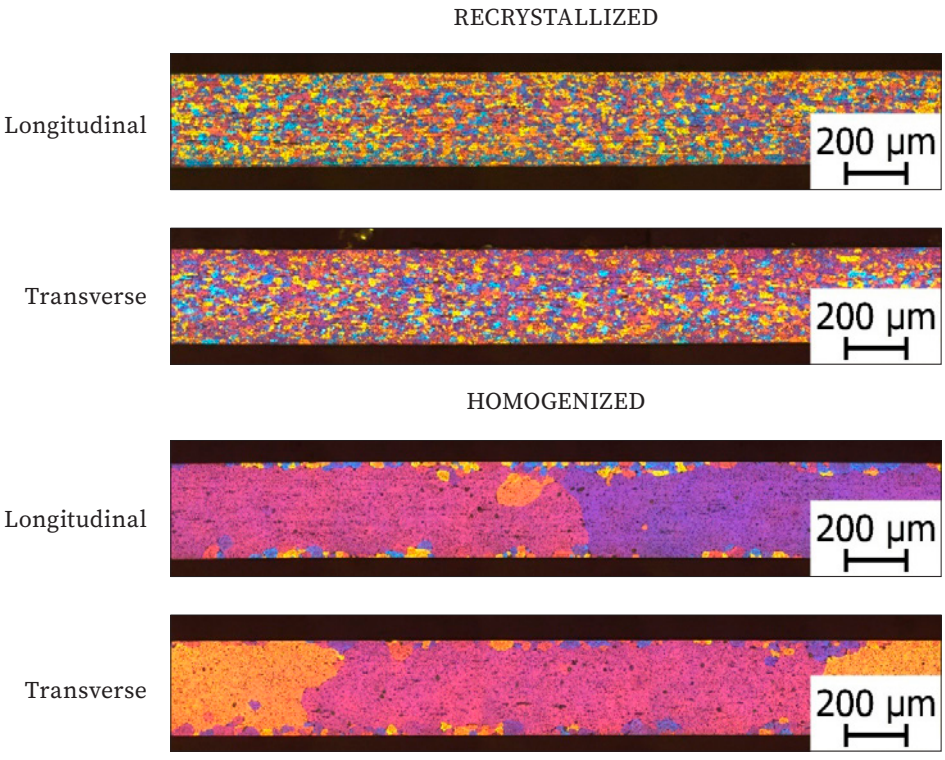

Fig. 12. Grain structure of low-alloyed EN AW-8011

Table 4. Average grain size of the recrystallized and homogenized samples

Variant	Heat-treatment	Direction	Average grain size [μm]
High-alloyed	RECRYSTALLIZED	longitudinal	12
		transverse	13
	HOMOGENIZED	longitudinal	20
		transverse	20
Low-alloyed	RECRYSTALLIZED	longitudinal	12
		transverse	12
	HOMOGENIZED	longitudinal	88
		transverse	103

4. Conclusions

The above-presented results justified the formulation of the following conclusions:

- Increased manganese and magnesium contents could be responsible for the higher strength properties of the high-alloyed sample of EN AW-8011.
- Both manganese and magnesium seemed to remain in the solid solution. This fact should be verified further, using superior detection techniques.
- The homogenized low-alloyed sample of EN AW-8011 revealed significantly greater elongation than that observed in relation to the homogenized high-alloyed sample of EN AW-8011. The probable reason could be the larger grain size.
- The surface of the homogenized high-alloyed samples was significantly darker than that of the low-alloyed homogenized sample (probably because of the presence of magnesium oxide in the surface layer).

Acknowledgements

The research work was supported by AL INVEST Břidličná, a.s. company (department of Research and Development).

REFERENCES

[1] J. R. Davis, Aluminum and aluminum alloys, ASM international, 1993.
[2] ČSN EN 573-3+A1: Hliník a slitiny hliníku – Chemické složení a druhy tvářených výrobků: Část 3: Chemické složení a druhy výrobků. 01/2023, 2023
[3] J. A. Green, Aluminum recycling and processing for energy conservation and sustainability, ASM International, 2007.
[4] K. M. McHugh, J. P. Delplanque, S. B. Johnson, E. J. Lavernia, Y. Zhou, Y., Y. Lin, Spray rolling aluminum alloy strip. Materials Science and Engineering: A, 383(1). 96–106 (2004). DOI: https://doi.org/10.1016/j.msea.2004.02.041
[5] J. Arbeiter, M. Vončina, D. Volšak, J. Medved, Evolution of Fe-based intermetallic phases during homogenization of Al–Fe hypoeutectic alloy. Journal of Thermal Analysis and Calorimetry, 142(5), 1693–1699 (2020). DOI: https://doi.org/10.1007/s10973-020-10161-8
[6] A. U. Malcioglu, C. Dogan, C. Inel, C. Gode, Effects of casting speed on thin gauge foil surface quality of 8079 aluminum alloy produced by twin roll casting method. Transactions of the Indian Institute of Metals, 72, 1001–1011 (2019). DOI: https://doi.org/10.1007/s12666-019-01563-w
[7] M. Vončina, K. Kresnik, D. Volšak, J. Medved, Effects of homogenization conditions on the microstructure evolution of aluminium alloy EN AW 8006. Metals, 10(3), 419 (2020). DOI: https://doi.org/10.3390/met10030419
[8] L. Kuchař, J. Drápala, Binární systémy hliník-příměs a jejich význam pro metalurgii, Děčín, 2003.
[9] Š. Michna, Encyklopedie hliníku, Prešov, 2005.
[10] M. Vončina, J. Medved, M. Steinacher, K. Ozimič, The influence of La and Ce additions on the solidification of alloys from the Al–Fe system. Journal of Thermal Analysis and Calorimetry, 1–10 (2024). DOI: https://doi.org/10.1007/s10973-024-13009-7
[11] J. H. Ryu, Y. S. Lee, D. N. Lee, The effect of precipitation on the evolution of recrystallization textures in an AA 8011 aluminum alloy sheet. Metals and Materials International, 7, 251–256 (2001). DOI: https://doi.org/10.1007/BF03026983
[12] C. Shi, K. Shen, Twin-roll casting 8011 aluminium alloy strips under ultrasonic energy field. International Journal of Lightweight Materials and Manufacture, 1(2), 108–114 (2018). DOI: https://doi.org/10.1016/j.ijlmm.2018.06.001
[13] R. E. Sanders Jr., Continuous casting for aluminum sheet: a product perspective. JOM, 64(2), 291–301 (2012). DOI: https://doi.org/10.1007/s11837-012-0247-y
[14] H. L. Chen, A. Jansson, Phase formation in A3003 alloys. Materials Today: Proceedings, 10, 296–305 (2019). DOI: https://doi.org/10.1016/j.matpr.2018.10.409
[15] A. Kagawa, Y. Tabira, Solute partitioning, liquidus and eutectic temperatures in freezing aluminium alloys. Materials Transactions, JIM, 32(11), 1076–1081 (1991). DOI: https://doi.org/10.2320/matertrans1989.32.1076
[16] E. Janssen, Chemical characterization of industrial steel and aluminium sheet surfaces by secondary ion mass spectrometry, glow discharge optical spectroscopy and other surface-sensitive techniques. Materials Science and Engineering, 42, 309–320 (1980). DOI: https://doi.org/10.1016/0025-5416(80)90040-3
[17] ČSN EN ISO 6892-1: Kovové materiály-Zkoušení tahem-Část 1: Zkušební metoda za pokojové teploty, 1999.
[18] ASTM E112-10: Standard Test Methods for Determining Average Grain Size, 2010.